JOURNAL OF MATERIALS SCIENCE 31 (1996) 1821–1828

Infrared infiltration and properties of SCS–6/Ti alloy composites

S. G. WARRIER, R. Y. LIN
Department of Materials Science and Engineering, University of Cincinnati, Cincinnati, OH 45221, USA

Liquid infiltration processes are seldom used in the fabrication of titanium matrix composites primarily because of severe interfacial reactions during processing. To minimize fibre–matrix interfacial reactions, a rapid infrared manufacturing (RIM) process has been developed. In this study, SCS-6 fibre reinforced titanium matrix composites were fabricated by the RIM process. Experimental results indicate that composites prepared by the RIM process exhibit small interfacial reaction zones and superior mechanical properties compared to diffusion bonded composites. Interfacial reactions during processing in this composite system have been investigated. Microscopic analyses showed that the carbon-rich coating present on SCS-6 fibres partially dissolved in the alloy during infiltration without forming a continuous reaction product. A physical model has been proposed to explain the dissolution mechanism of the carbon-rich coating. The dissolution rate of the coating at the processing temperature of 1300 °C was calculated to be 1.4×10^{-6} cm s^{-1}.

1. Introduction

Titanium matrix composites are potential candidates for structural application in the aerospace industry primarily because of their high specific strength and modulus, good dimensional stability and retention of strength at elevated temperatures. These composites are commonly fabricated by solid state diffusion bonding processes such as vacuum hot pressing or hot isostatic pressing using either metallic foils [1] or powder cloths [2] layered alternately between fibre preforms, or plasma spraying fibre–matrix preforms followed by vacuum hot pressing [3]. However, long processing times at elevated temperatures in these processes often result in extensive interfacial reactions in as-fabricated composites. Furthermore, high operating costs, expensive pressing equipment and vacuum requirements make these diffusion bonded composites too expensive for most industrial applications. One solution to the above problem is liquid infiltration which offers low costs, near net shape fabricability, process versatility and high fibre volume fractions. However, because of the severity of the reaction between liquid titanium and the reinforcing fibres, this technique has not received much attention in the manufacture of titanium matrix composites. The literature survey reveals only one attempt by Toloui [4] to fabricate carbon fibre reinforced titanium alloy composites by the liquid infiltration technique. Toloui [4] attempted to prepare carbon fibre reinforced titanium alloy composites using induction heating. Composites fabricated by him exhibited severely degraded fibres and very poor mechanical properties.

In order to ensure the success of the liquid infiltration process for the fabrication of titanium matrix composites, methods of minimizing the reaction between fibres and the matrix during processing must be developed. These may include shortening the processing time, applying protective coatings on reinforcement fibres, or incorporating alloying elements that retard the reaction. In an effort to reduce the processing time, a pressureless liquid infiltration process employing infrared heating, rapid infrared manufacturing (RIM), for fabricating titanium and aluminium matrix composites has been developed at the University of Cincinnati [5–10].

Infrared heating has significant advantages over conventional heating techniques for fabricating metal matrix composites. Rapid heating, instantaneous starting and stopping, precise control of temperature and low operating costs are some of the features where infrared heating has a significant edge over conventional resistance and induction heating. Due to differences in infrared absorption characteristics of different materials, selective heating of the crucible and the composite lay-up can be achieved without heating the furnace walls. Thus, heating and cooling rates as high as 200 °C s^{-1} may be obtained during fabrication. With such high temperature ramping capabilities, the entire composite fabrication process can be completed in only 1–2 min as opposed to several hours in conventional diffusion bonding techniques. Due to short processing times, reactions at the fibre–matrix interface of highly reactive systems such as SiC–Ti can be effectively controlled. Another major advantage of the fast heating rate is reduced oxidation which results in enhanced wetting characteristics and flow properties of the liquid alloy. The lack of oxidation and the inherent low viscosity of liquid metals (typically

0022–2461

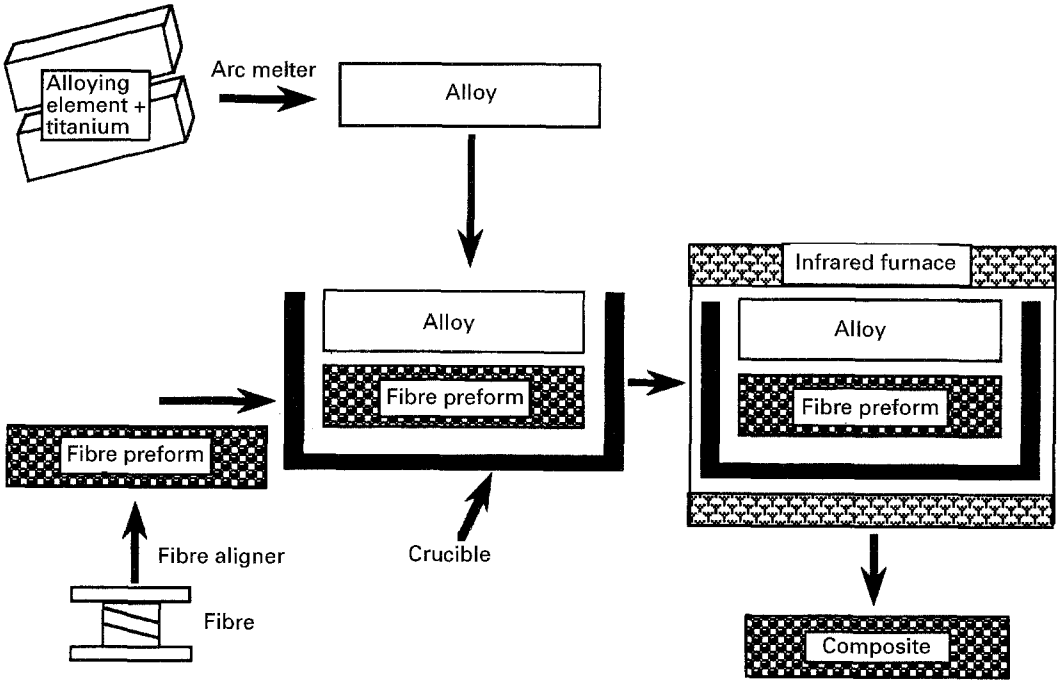

Figure 1 Schematic representation of the rapid infrared manufacturing process.

around 10^{-2} poise, similar to that of water) [11] permit infiltration of fibre preforms, up to 4 plies in thickness, in times shorter than a second. From an economic point of view, fast heating eliminates the requirement of vacuum. Also, fast heating reduces the amount of phase separation when heating through a two phase region. As a result, the effect of partial melting is minimized which further improves wetting and flow characteristics.

In this study, interfacial reactions between a liquid titanium alloy and SCS-6 fibres have been investigated. Results have been used to determine composite fabrication feasibility. Reaction characteristics will be explained from thermodynamic and kinetic stand points. Mechanical properties of rapid infrared manufactured composites will also be addressed.

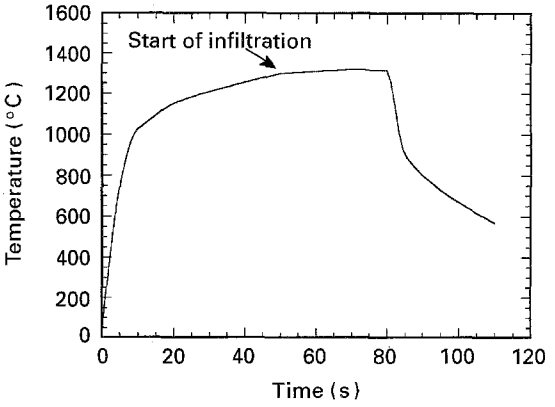

Figure 2 Temperature of the crucible as a function of time during the rapid infrared manufacturing process. Processing conditions: 1300 °C for 30 s.

2. Experimental techniques

2.1. Composite fabrication

Composites used in this study were fabricated by the rapid infrared manufacturing process. A sketch of the process is shown in Fig. 1. The fibres used were continuous SiC fibres (SCS-6) from Textron Specialty Materials. These fibres were cut and aligned into preforms which were stacked unidirectionally in high purity graphite crucibles. Graphite screws were used to prevent the fibres from floating up. The matrix was a titanium–nickel alloy containing 80 wt % Ti, designated as Ti80, prepared by conventional vacuum arc melting. The alloy was cut to the required size and placed in the graphite crucible on top of the fibres in an infrared furnace. The temperature was controlled with a R-type thermocouple attached to a tantalum sheet placed underneath the graphite crucible and monitored with a thermocouple spot welded on the alloy. This lay up was heated at rates of 100–200 °C in a flowing argon environment to temperatures above the melting point of the alloy for infiltration.

Samples with fibre volume fractions up to 23% and sizes up to 75 mm × 13 mm × 3 mm, were fabricated by the RIM process at temperatures of 1300–1350 °C and holding times of 5–30 s. Fig. 2 shows a typical time–temperature curve for a composite fabricated by the RIM technique. As observed from the figure, the heating and cooling cycle as well as the holding time are extremely short. After infiltration, the composite was extracted from the graphite crucible by rough grinding with SiC papers. They were then polished to a 600 grit finish for flexural testing at room temperature. For microscopic analysis, composites with a fibre volume fraction of 5%, were fabricated by the rapid infrared manufacturing process at 1300 °C for 1, 5, 25, 60, 120 and 180 s. These composites were prepared for electron microscopic analysis.

2.2. Mechanical testing

The flexural properties of composites were measured by using a three-point bend set-up on an Instron

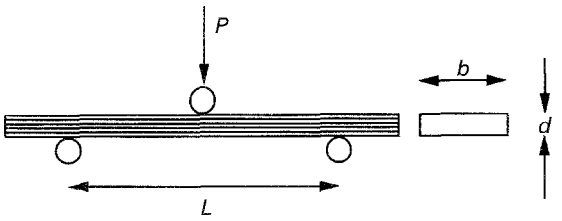

Figure 3 Set-up for testing flexural properties of composites.

testing machine connected to a data acquisition system. The testing was done in accordance with ASTM specification D-790-86 [12]. A span to depth ratio (L/d) of 30 was maintained. The load was applied perpendicular to the fibres causing tensile stresses to develop along the fibre axis on the outer surface of the composite. The flexural testing set-up is shown in Fig. 3. The maximum flexural strength (σ_{max}) and modulus (E) of the composites were determined from [13]:

$$\sigma_{max} = 3PL/2bd^2 \quad (1)$$

and

$$E = PL^3/4bd^3\delta, \quad (2)$$

where P is the applied load, L is the span, b and d are the width and the thickness of the sample, respectively, and δ is the centre displacement at fracture. The fracture surface was examined under a scanning electron microscope (SEM) to determine the mode of failure in the composites.

2.3. Sample preparation and microscopic analysis

In order to study the interfacial reaction characteristics of as-processed samples, all samples were cut perpendicular to the fibre axis with a slow speed diamond saw. They were mounted and polished with diamond pastes to a 1 μm finish. The samples were etched with Kroll's reagent (1–3 ml HF, 2–6 ml HNO_3 in 100 ml H_2O) for 5 s and observed under an optical microscope. They were then sputter coated with silver and viewed under a scanning electron microscope (SEM) with an energy dispersive X-ray (EDX) analysis facility.

3. Results

3.1. Composite cross-section and wetting characteristics

The cross-section micrographs of SCS-6 fibre reinforced titanium alloy matrix composites are shown in Fig. 4. The composites were well wetted, fully dense and had good fibre distribution with limited interfacial reaction. The excellent wetting characteristics are evident from the cross-section of a 48 vol % SCS-6/Ti80 composite, Fig. 4c, in which the alloy has flowed in between fibres that were in close proximity to each other. The average thickness of the reaction product in rapid infrared manufactured composites was about 1 μm. Conversely, in SCS-6/Ti–24Al–11Nb composites produced by the powder cloth diffusion bonding technique, the reaction zone thickness was about 2 μm [14] and in SCS-6/Ti–48Al–1Ta composites produced by hot pressing, it was about 5 μm [15]. The unreacted pyrocarbon coating in SCS-6/Ti alloy composites prepared by the RIM technique was in the order of 2 μm which is comparable to the coating thickness observed in conventional diffusion bonded SCS-6/Ti–6Al–4V composites [16].

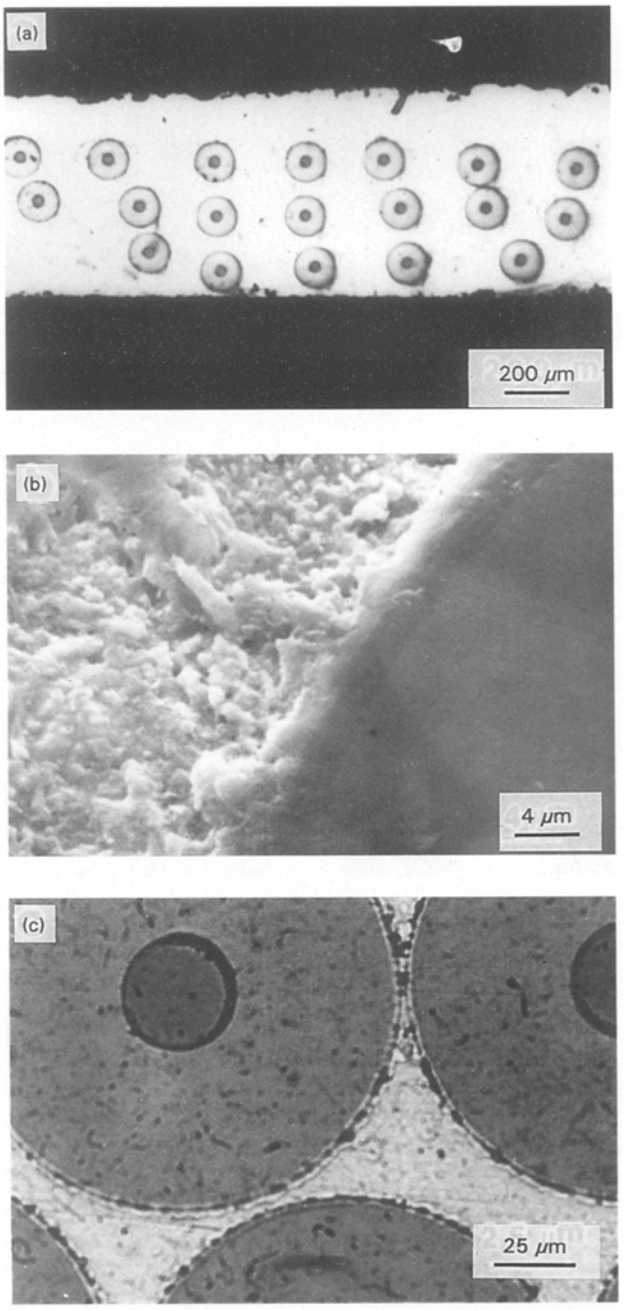

Figure 4 Micrographs of cross-sections of SCS-6/Ti composites fabricated by the rapid infrared manufacturing process: (a) and (b) showing no voids, good fibre distribution and limited interfacial reaction, and (c) showing excellent wetting characteristics.

3.2. Mechanical properties

The flexural strength and modulus of the composites and the alloy are listed in Table I along with the tensile strength and modulus of the fibre and those of some of

TABLE I Mechanical properties of fibres, titanium alloys and composites

Material	Strength (MPa)	Modulus (GPa)	Reference
SCS-6 fibre	3950	400	[17]
Ti80 (as-cast)	1290	118	[a]
SCS-6 (23 vol %)/Ti80	1734	195	[a]
Ti–6Al–4V	890	110	[18]
SCS-6 (35 vol %)/Ti-6-4	1455	225	[18]
SCS-6 (35 vol %)/Ti-6-4	1690	186	[19]
SCS-6 (38–41 vol %)/Ti-15-3	1951	213	[19]
SCS-6 (35 vol %)/Ti-2411	1183	184	[14]

[a] Test results from this laboratory.

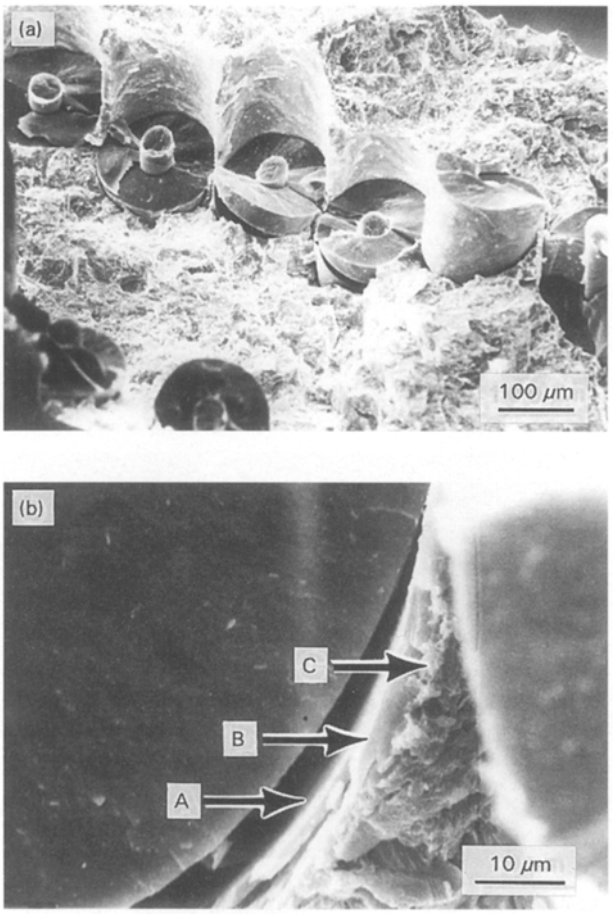

Figure 5 Secondary electron images of the fractured surface of SCS-6 fibre reinforced Ti80 composites fabricated by the rapid infrared manufacturing process. "A" represents the debonded surface of the coating, "B" represents the carbon-rich coating and "C" represents the reaction product.

the titanium matrix composites reported in the literature [14, 17–19]. As shown in Table I, SCS-6/Ti80 composites fabricated by the RIM technique exhibit strengths and moduli comparable to SCS-6/Ti alloy matrix composites made with diffusion bonding.

The modulus and specific modulus of 23 vol % SCS-6/Ti80 composites were, respectively, 1.7 and 1.8 times that of the alloy. The rule of mixtures (ROM) modulus was 183 GPa. The observed modulus in these composites was approximately 100% ROM modulus. The strength and specific strength of these composites were, respectively, 1.1 times and 1.2 times that of the alloy. The strength of the composite was 81% ROM value.

Examination of the fractured surface in these composites revealed both fibre pull out and debonding (Fig. 5). Fibre debonding occurred at two locations: (a) between the SiC fibre and the carbon-rich coating, and (b) between the inner carbon core and the SiC fibre. High magnification SEM image of the debonded area at the fibre-matrix interface (Fig. 5b) shows that the reaction product adhered well to the matrix and that debonding occurred between the fibre and the carbon-rich coating. In addition to fibre debonding, several fibres appeared to have cracked in multiple areas. The presence of cracks along with debonding suggests that the interface was reasonably strong and that debonding occurred at a stress close to the fibre breaking stress.

3.3. Interface analysis

SEM secondary electron image, back scattered image and EDX spectrographs of the interface in SCS-6/Ti80 composites, processed at 1300 °C for 25 s, are shown in Fig. 6. It can be observed from the secondary electron image (Fig. 6a) that the fibres reacted with the alloy and formed a non-uniform layer of the reaction product. High magnification micrographs of the reaction zone (Fig. 6c) showed that the reaction product was not a dense continuous layer. The back scattered image of the interface (Fig. 6b) showed that the reaction product was darker than the unetched phases and precipitates, and thus, consisted of lighter elements. EDX analysis was done at the interface and the surrounding areas. The specimen was probed at the fibre coating, at the reaction zone, and at distances of 5 and 50 μm from the outer surface of the reaction zone. The results of the EDX analysis are presented in Fig. 7 and Table II. As shown in the table, the coating consisted of mainly silicon, indicating insignificant diffusion of titanium into the fibres. The reaction product consisted of primarily titanium with small amounts of silicon and nickel suggesting that the reaction product is TiC. The presence of small amounts of silicon and nickel in the spectrograph of the reaction product is believed to be the effect of signal pick up from areas outside the reaction zone due to a relatively larger spot size than the reaction zone. EDX analyses at distances of 5 and 50 μm from the interface revealed similar amounts of nickel and traces of silicon.

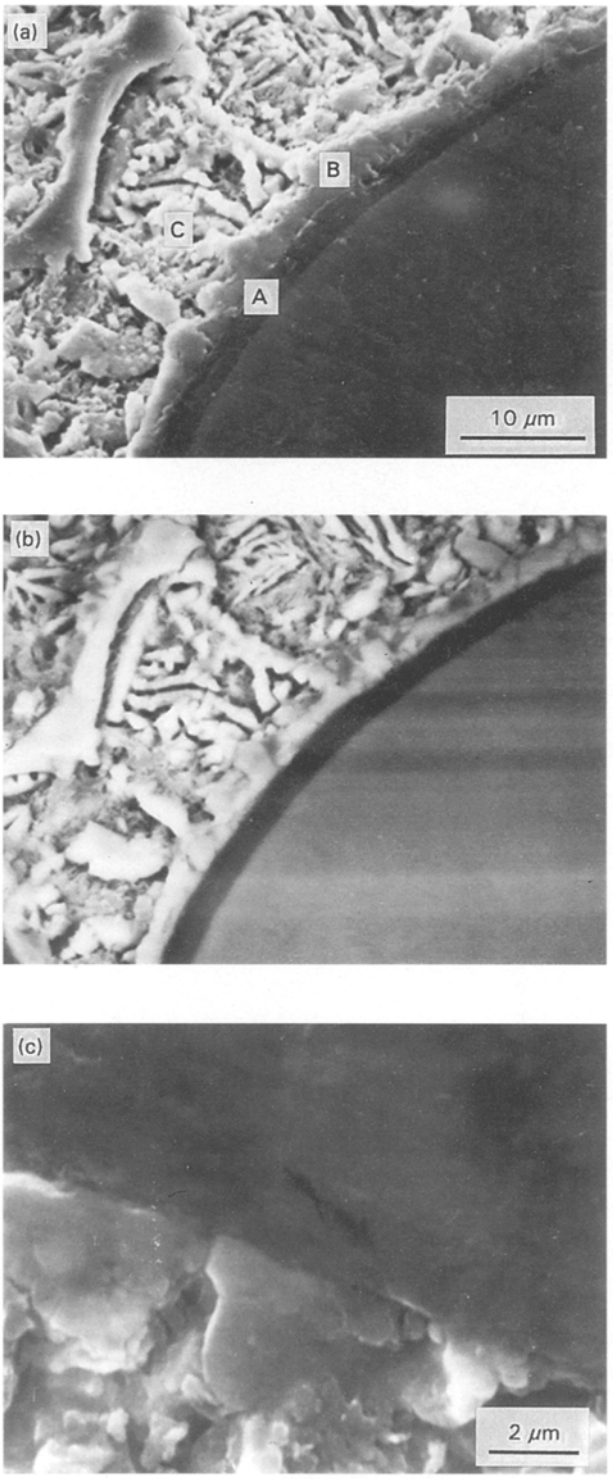

Figure 6 The interface in SCS-6 fibre reinforced Ti80 composites: (a) secondary electron image, (b) back scattered image, and (c) high magnification secondary electron image. "A" represents the coating, "B" represents the reaction product and "C" represents the matrix.

SEM secondary electron images of interfaces in SCS-6/Ti80 composites processed at 1300 °C for different times ranging from 1 to 120 s are shown in Fig. 8. In order to analyse the reaction after the coating had been consumed, SCS-6 fibre reinforced

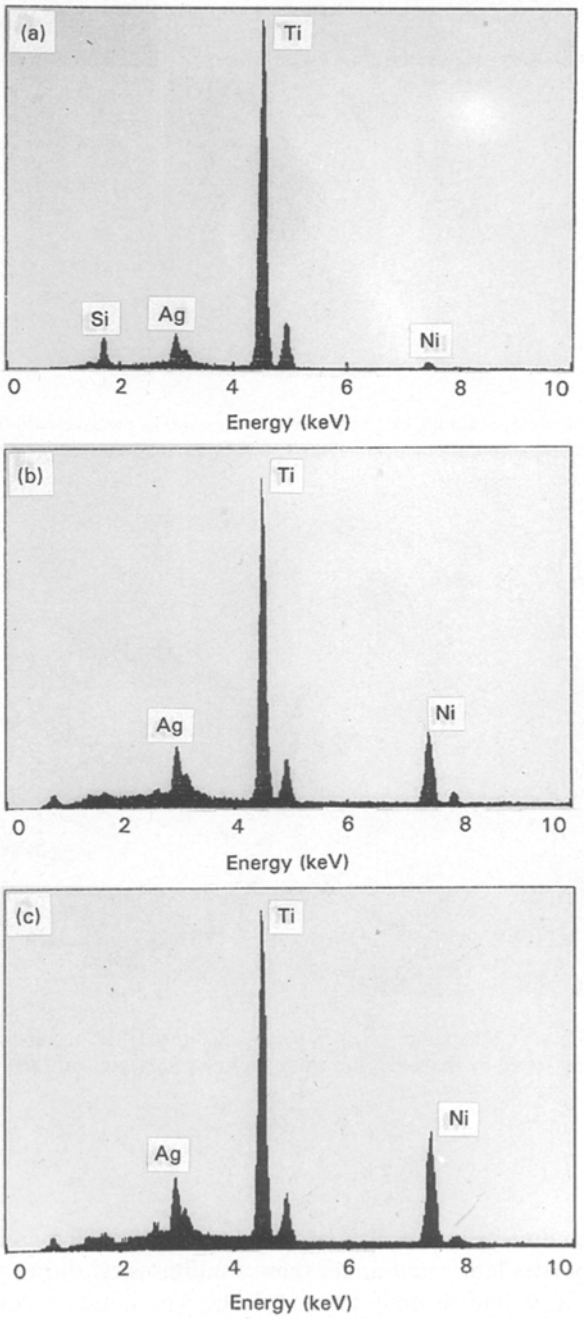

Figure 7 EDX spectrograph of SCS-6/Ti composites: (a) at the reaction product, (b) at a distance of 5 μm from the reaction zone, and (c) at a distance of 50 μm from the reaction zone.

TABLE II EDX analysis of the interface in SCS-6/Ti80 composites

Position in fig. 6a	Elements			Comments
	Titanium	Silicon	Nickel	
at coating (A)	~ 7 wt %	~ 90 wt %	Traces	negligible Ti diffusion
at r.z. (B)	~ 88 wt %	~ 3 wt %	< amount in alloy	r.z. is TiC*
5 μm away (C)	~ 60 wt %	traces	~ amount in alloy	no segregation
50 μm away	~ 64 wt %	traces	~ amount in alloy	no segregation

*r.z. is reaction zone.

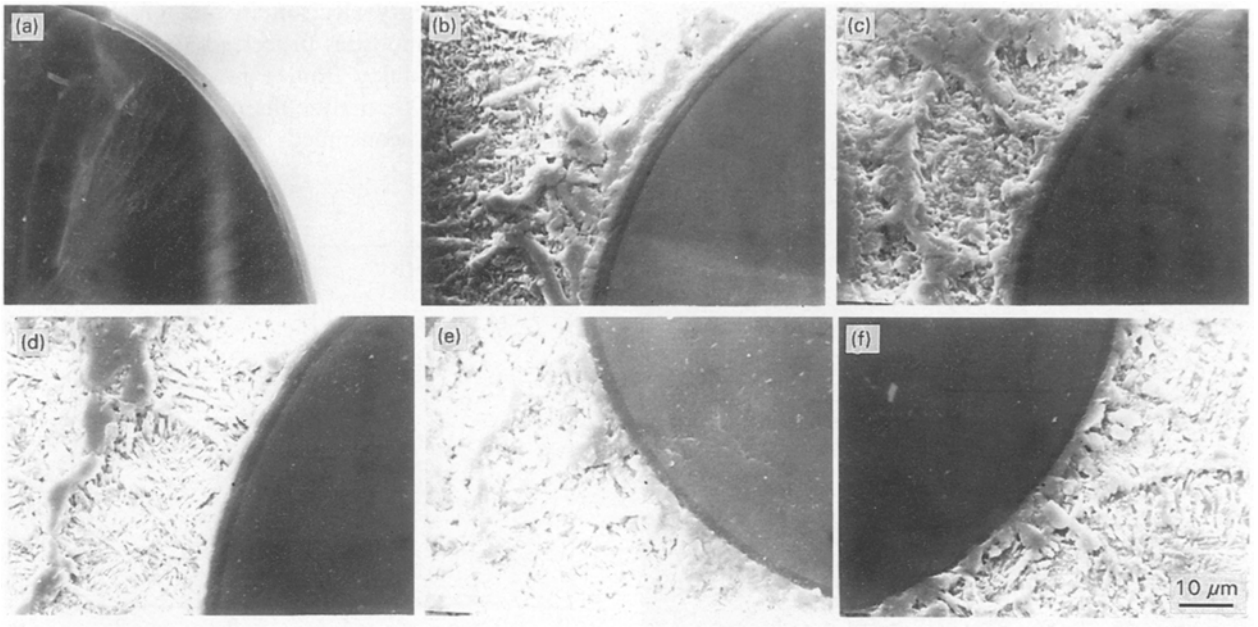

Figure 8 Scanning electron micrographs of (a) as received SCS-6 fibres and (b)–(f) interfaces in composites fabricated by the rapid infrared manufacturing process at 1300 °C for (b) 1 s, (c) 5 s, (d) 25 s, (e) 60 s and (f) 120 s.

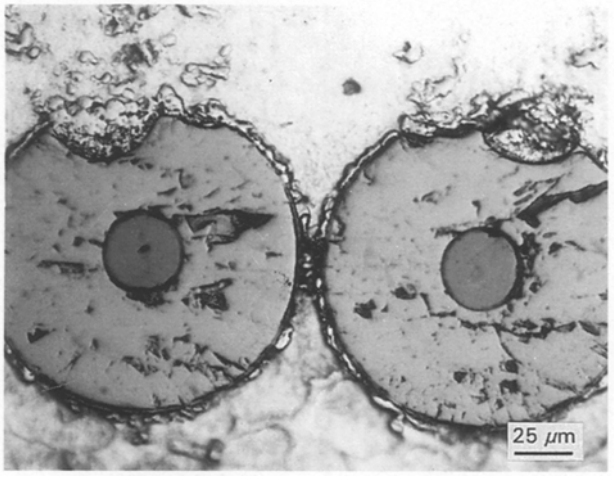

Figure 9 Micrograph of SCS-6 fibre reinforced Ti80 composite fabricated by the rapid infrared manufacturing process at 1300 °C for 180 s.

composites were also processed for 180 s. The composites fabricated under these conditions, as shown in Fig. 9, had severely reacted fibres. The interface consisted of scalloped interfaces that are characteristic of reactions in the SCS-0/Ti system [20].

The average thickness of both carbon-rich layer retained and TiC formed at different processing times were obtained by averaging over twenty measurements from different fibres. Fig. 10 plots the thickness of carbon coating retained versus processing time. As seen from the figure, except the initial steep drop, the reduction in coating thickness varies linearly with processing time. Fig. 11 shows the thickness of TiC formed as a function of processing time. Here too, except the initial deviation, the average thickness of TiC appears to follow a linear growth rate.

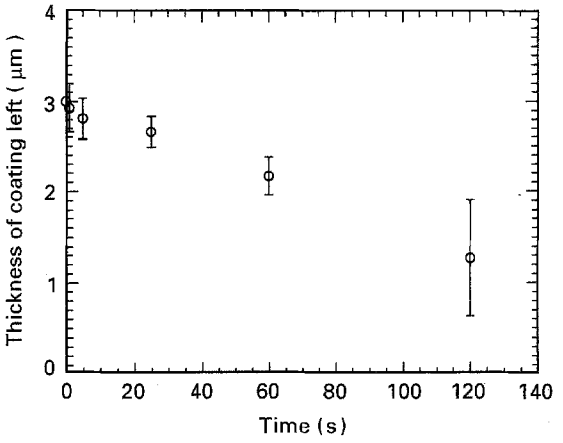

Figure 10 Plot of the thickness of the carbon-rich coating left on the SCS-6 fibre surface as a function of processing time.

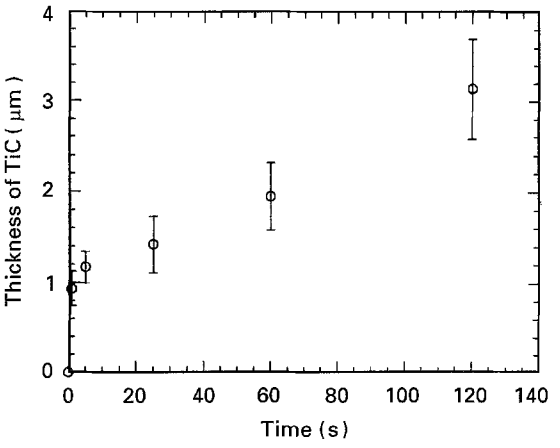

Figure 11 Plot of the thickness of TiC formed on the fibre surface as a function of processing time.

4. Discussion

In order to explain the observed dissolution process, thermodynamic and kinetic aspects of fibre–matrix interactions in the composite system were evaluated.

4.1. Thermodynamic consideration

Ning and Pirouz [21] studied the coating on SCS-6 fibres using transmission electron microscopy and electron energy loss spectroscopy (EELS). They observed that the outer coating consisted of SiC particles embedded in a carbon matrix. There was no free silicon observed in the coating. The chemical composition of the outer coating was also studied by Lancin *et al.* [22] using secondary ion mass spectroscopy (SIMS). They reported that, starting from the SiC fibre and moving towards the surface, with the exception of a few small peaks, the silicon concentration gradually decreased to zero. The study by Lancin *et al.* was done on SCS-6 fibres embedded in a titanium matrix by diffusion bonding. For a diffusion bonding process, since heating at high temperatures is needed for several hours, it is likely that silicon redistribution could have occurred during fabrication. On the other hand, the infrared processing technique is comparatively very fast. Hence, silicon redistribution is unlikely to have occurred to any significant level. Thus, the microstructure reported by Ning and Pirouz [21] is believed to be valid for analysis in this study. Since there is no free carbon or silicon in the SiC particles and no free silicon in the carbon matrix, the interaction between liquid titanium and the coating may be estimated from the thermodynamic conditions that exist between SiC and liquid titanium and that between carbon and liquid titanium.

An earlier study by the authors with the SCS-0 (stoichiometric SiC fibres)–liquid titanium system [20] indicated that SiC fibres are unstable in the presence of liquid titanium and dissociates into Si and C dissolved in the alloy. In these composites, a continuous layer of reaction products did not form at the fibre surface and large amounts of fibres dissolved in the alloy. Studies with the carbon fibre–liquid titanium system [7, 8] indicated that, during infiltration, a continuous layer of TiC formed at the fibre surface. Thus, during interactions between the coating on SCS-6 fibres and the liquid alloy, SiC particles would dissolve in the alloy, whereas, carbon particles would react to form TiC. As soon as the coating is completely dissolved, the fibres would act as SCS-0 fibres and dissolution would occur without the formation of continuous reaction products at the interface.

4.2. Kinetic consideration

From the work done by Ning and Pirouz [21], the volume fraction of SiC particles as a function of the coating thickness in SCS-6 fibres can be plotted as shown in Fig. 12. From this figure, it can be noted that the volume fraction of SiC may be as high as 65% at both the outer surface of the coating and at 1.5 μm from the surface. The average volume fraction of SiC particles over the whole coating thickness is as high as 45% and at the middle 100 nm of the carbon coating, it is about 12%. Thus, it is likely that a significant amount of SiC grains would be in touch with each other and may form a continuous path of dissolution. In the outermost 1.5 μm layer of the coating, the volume fraction of the SiC particles decreases with

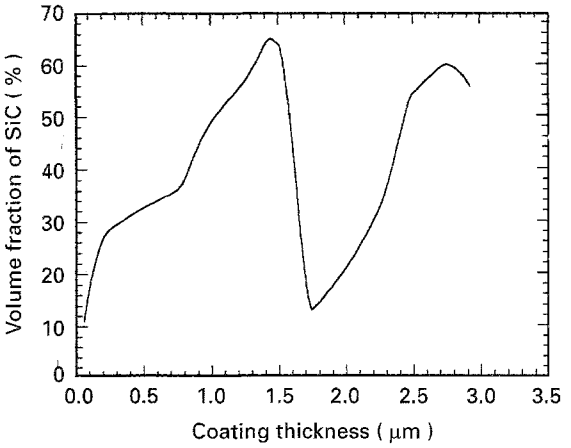

Figure 12 Volume fraction of SiC as a function of coating thickness on SCS-6 fibres, calculated from data in [21].

increasing distance from the outer surface. Ning and Pirouz also observed that within this 1.5 μm layer, the particle size increases with the distance from the outer surface. Thus, the spacing between SiC particles increases as the fibre coating is consumed and, as a result, continuous channels of dissolution may become less feasible as the interaction proceeds. In the event that the dissolution channels get blocked by a continuous layer of TiC (most probably when the dissolution front reaches the middle layer of the coating), small amounts of TiC dissolution can occur which may re-open the channels. As a result, dissolution of the coating occurs without the formation of a continuous reaction product.

A process simultaneously occurring is the formation of TiC due to the reaction between liquid titanium and free carbon in the coating. In the initial regions of the coating, since large amounts of SiC particles exist, TiC formed is in the form of small precipitates attached to the surface of the coating. Since dissolution of SiC occurs around these TiC particles, they disconnect from the fibre surface, migrate away and agglomerate. The SiC interparticle spacing within the outermost 1.5 μm layer increases as the dissolution proceeds and, as a result, the probability of the separation of large chunks of TiC from the fibre surface as well as the formation of a continuous TiC layer may increase. If a continuous layer of TiC forms, as stated earlier, small amounts of TiC dissolution can occur which will re-open the channels. Thus, TiC grows as a discontinuous layer rather than a continuous dense one, and both, coating dissolution and TiC growth occurs linearly with time.

In the uncoated SiC fibre (SCS-0) reinforced composites, an earlier study [20] indicated that the dissolution of the fibres occurred by two distinct mechanisms: (a) uniform fibre attack as a result of general dissolution and (b) scalloped fronts due to active dissolution. The uniform dissolution is believed to have occurred by an isothermal dissolution mechanism, whereas, scalloped interfaces are believed to have formed by a self sustained active dissolution mechanism caused by localized heating. During the

fabrication of SCS-6 fibre reinforced composites, an active dissolution mechanism caused by localized heating may not occur due to the presence of irregular channels of SiC which increase heat dissipation due to a large specific surface area. Thus, the dissolution of SiC particles in the carbon-rich coating is believed to occur isothermally. Once the coating is dissolved, the SCS-6 fibres are essentially SCS-0 fibres and the self sustained active dissolution mechanisms becomes operative.

The dissolution rate of the coating calculated from Fig. 10 is 1.4×10^{-6} cm s^{-1}. This rate is about 4 times lower than the uniform fibre dissolution rate in SCS-0/Ti composites [20]. This difference is not significant enough to confirm the effect of free carbon on the dissolution rate. Also observed from the figure, composites processed at 120 s have a large standard deviation with the error bars extending to near zero coating thicknesses. Since completely reacted coatings may cause destructive interactions between the fibre and the alloy, weak spots can develop. Therefore, processing times above 120 s may be detrimental to the mechanical properties of the composite. The TiC growth rate was calculated from Fig. 9 as 1.7×10^{-6} cm s^{-1}. The linear variation of TiC thickness with time suggests that a continuous layer of TiC does not form, and as a result, the process is not controlled by the diffusion of elements across the reaction product. Discontinuous large particles of TiC support the hypothesis of TiC agglomeration of small particles initially formed at different sites.

5. Conclusions

SCS-6 fibre reinforced titanium alloy matrix composites fabricated by the rapid infrared manufacturing process exhibited small well-controlled interfacial reaction and good mechanical properties. Thermodynamic analysis indicated that, during fabrication, SiC particles present in the coating would dissolve in the liquid alloy and carbon particles would form TiC. A physical model has been proposed to explain the dissolution mechanism in SCS-6 fibre reinforced composites. The model suggests that, due to the large amounts of SiC particles in the coating, continuous dissolution channels are formed. These channels result in the dissolution of the coating without the formation of a continuous reaction product at the fibre surface. Due to the absence of a continuous reaction layer, the rate of both coating dissolution and TiC growth varies linearly with time. The coating dissolution rate was 1.4×10^{-6} cm s^{-1} and the TiC growth rate was 1.7×10^{-6} cm s^{-1}. After the carbon-rich coating was completely dissolved, the SCS-6 fibres behaved as SCS-0 fibres and scalloped dissolution fronts developed.

High reaction rates observed in the SCS-6/Ti80 composite system indicate that for the successful implementation of liquid infiltration for the fabrication of titanium matrix composites, the process should be completed in a short time. Processes such as rapid infrared manufacturing provide such conditions.

Acknowledgements

The authors would like to acknowledge the support from NASA Space Engineering Research Center at the University of Cincinnati and Edison Materials Technology Center. The authors would also like to thank Mr M.A. Mittnick of Textron Specialty Materials for supplying the fibres.

References

1. P. MARTINEAU, R. PAILLER, M. LAHARE and R. NASLAIN, *J. Mater. Sci.* **19** (1984) 2749.
2. P. K. BRINDLEY, in "High Temperature Ordered Intermetallic Alloys II", edited by N. S. Stoloff, C. C. Koch, C. T. Liu and O. Izumi (MRS, Pittsburgh, PA, 1987) p. 419.
3. A. M. RITTER, E. L. HALL and N. LEWIS, in "Intermetallic Matrix Composites", edited by D. L. Anton, P. L. Martins, D. B. Miracle and R. McMeeking (MRS, Pittsburgh, PA, 1990) p. 413.
4. B. TOLOUI, *ICCM-V* **1** (1985) 773.
5. S. G. WARRIER, C. A. BLUE and R. Y. LIN, *J. Mater. Sci. Lett.* **12** (1993) 865.
6. S. G. WARRIER and R. Y. LIN, *Scripta Metall. Mater.* **28** (1993) 313.
7. *Idem, JOM*, **45** (1993) 24.
8. *Idem, Scripta Metall. Mater.* **29** (1993) 147.
9. *Idem, ICCM IX* **1** (1993) 720.
10. *Idem, Scripta Metall. Mater.* **29** (1993) 1513.
11. A. MORTENSEN, J. A. CORNIE and M. C. FLEMINGS, *J. Met.* **40** (1988) 12.
12. "Annual Book of ASTM Standards", edited by R. A. Storer, sec. 8, Vol. 08.01, (American Society for Testing and Materials, Philadelphia, PA, 1989) p. 280.
13. L. A. CARLSSON and R. B. PIPES, in "Experimental Characterization of Advanced Composite Materials" (Prentice Hall Inc., Englewood Cliffs, NJ, 1987) p. 89.
14. P. K. BRINDLEY, S. L. DRAPER, M. V. NATHAL and J. L. ELDRIDGE, in "Fundamental Relationships Between Microstructure and Mechanical Properties of Metal Matrix Composites", edited by P. K. Liaw and M. N. Gungor (TMS, Warrendale, PA, 1990) p. 387.
15. S. KRISHNAMURTHY, in "Interfaces in Metals-Ceramics Composites", edited by R. Y. Lin, R. J. Arsenault, G. P. Martins and S. G. Fishman (TMS, Warrendale, PA, 1990) p. 75.
16. C. JONES, C. J. KIELY and S. S. WANG, *J. Mater. Res.* **5** (1990) 1435.
17. T. SCHOENBERG, in "Engineering Materials Handbook-Composites", Vol. 1, edited by T. J. Reinhart (American Society for Metals, Metals Park, OH, 1987) p. 58.
18. P. R. SMITH, F. H. FROES and J. T. CAMMETT, in "Mechanical Behavior of Metal Matrix Composites", edited by J. E. Hack and M. F. Amateau (American Institute of Mining, Metallurgical and Petroleum Engineers, Warrendale, PA, 1983) p. 143.
19. "Continuous Silicon Carbide Metal Matrix Composites", (Textron Specialty Materials, Lowell, MA).
20. S. G. WARRIER and R. Y. LIN, *Metall. Mater. Trans.* **26A** (1995) 1885.
21. X. J. NING and P. PIROUZ, *J. Mater. Res.* **6** (1991) 2234.
22. M. LANCIN, J. S. BOUR, J. THIBAULT-DESSEAUX and N. VALIGNAT, *J. Microsc. Spectrosc. Electron.* **3** (1988) 503.

Received 22 December 1993
and accepted 16 August 1995